Journal of Inorganic Biochemistry 110 (2012) 83–93

Contents lists available at SciVerse ScienceDirect

Journal of Inorganic Biochemistry

journal homepage: www.elsevier.com/locate/jinorgbio

Focussed review

# Elucidating second coordination sphere effects in heme proteins using low-temperature magnetic circular dichroism spectroscopy

Nicolai Lehnert

*Department of Chemistry, The University of Michigan, 930 North University Avenue, Ann Arbor, MI 48109-1055, USA*

ARTICLE INFO

*Article history:*
Received 7 October 2011
Received in revised form 27 February 2012
Accepted 28 February 2012
Available online 10 March 2012

*Keywords:*
Heme proteins
Second coordination sphere effects
Hydrogen bonding
Magnetic circular dichroism spectroscopy
Cytochrome P450
Electronic structure

ABSTRACT

This paper reviews recent findings on how the second coordination sphere of heme proteins fine-tunes the properties of the heme active site via hydrogen bonding. This insight is obtained from low-temperature magnetic circular dichroism (MCD) spectroscopy. In the case of high-spin ferric hemes, MCD spectroscopy allows for the identification of a multitude of charge-transfer (CT) transitions. Using optically-detected magnetic saturation curves, out-of-plane polarized CT transitions between the heme and its axial ligand(s) can be identified. In the case of ferric Cytochrome P450cam, the corresponding $S(\sigma) \rightarrow Fe(III)$ CT transition can be used as a probe for the {Fe(III)–axial ligand} interaction, indicating that the hydrogen bonding network of the proximal Cys only plays a limited role for fine-tuning the Fe(III)–S(Cys) interaction. In the case of high-spin ferrous hemes with axial His/imidazole coordination, our MCD-spectroscopic investigations have uncovered a direct correlation between the strength of the hydrogen bond to the proximal imidazole ligand and the ground state of the complexes. With neutral imidazole coordination, the doubly occupied d-orbital of high-spin iron(II) is of $d_\pi$ character, located orthogonal to the heme plane. As the strength of the hydrogen bond increases, this orbital rotates into the heme plane, changing the ground state of the complex.



## 1. Introduction

*Second coordination sphere (SCS) effects* in proteins and transition metal complexes correspond to interactions of the metal center and its primary ligands with groups that are not part of the intimate coordination environment of the metal. In proteins, SCS effects are usually mediated by amino acid side chains in the substrate (active site) pocket of the protein. The most important types of interactions are hydrogen bonding, electrostatic (between charged groups) and dipole interactions, steric interactions, and π-stacking of aromatic side chains. These interactions are used by proteins for substrate recognition (binding and precise orientation in the active site), for fine-tuning of ligand donor strengths and redox potentials of transition metal centers, to enforce unnatural coordination geometries on transition metal complexes (the 'entatic' state), for proton and electron transfer, etc. [1]. The most important SCS interaction is hydrogen bonding. A famous example in this respect is the distal His in hemoglobin (Hb) and myoglobin (Mb), which forms a hydrogen bond to dioxygen bound to the heme center, and in this way, stabilizes the oxy-Hb/Mb complex [2].

SCS effects, in particular hydrogen bonding, are generally thought to be used in nature to fine-tune the properties of all heme protein active sites. This pertains particularly to hydrogen bonds to either the axial ligand(s) of heme, heme side chains, or substrates bound to the heme center. In this way, SCS effects allow principally similar active sites, like the {heme-thiolate(Cys)} active site in all members of the Cyt. P450 family or the {heme-imidazole(His)} active site in globins, (per)oxidases and heme sensor proteins, to perform a surprisingly diverse range of functions. This requires adjustments in the electronic structures, redox potentials, and reactivities of the {heme–axial ligand} (catalytic) units in these different proteins. Despite this central importance of hydrogen bonding for heme protein function, however, it has been found very difficult to obtain direct insight into how exactly hydrogen bonding affects the electronic structures and properties of heme protein active sites. For example, it has been observed frequently that changes in the hydrogen bonding network of axial ligands to heme can have a distinctive effect on redox potential [3–5], but it is not clear whether this relates to changes in heme–axial ligand bond strength, changes in ground state of the heme, changes in heme conformation, etc., and whether the ferrous or ferric oxidation state is primarily affected by the change (or both).

*Magnetic Circular Dichroism (MCD) spectroscopy* has long been used to elucidate the geometric and electronic structures of heme proteins [6–10]. In particular, MCD spectroscopy has been frequently applied as a 'finger-printing' technique to identify (a) the number and types of axial ligands bound to heme, (b) the oxidation and spin states of the heme, and (c) the heme conformation, in particular out-of-plane distortions of the heme. For example, in the low-spin ferric oxidation state of heme, low-energy (NIR) transitions are observed around 5000–10000 $cm^{-1}$ that are characteristic for the axial ligands of heme [6,11–13]. In addition, axial thiolate coordination is easily identified from the MCD spectra [14].

*E-mail address:* lehnertn@umich.edu.

0162-0134/$ – see front matter © 2012 Elsevier Inc. All rights reserved.
doi:10.1016/j.jinorgbio.2012.02.033

In order to utilize the full power of MCD spectroscopy, low-temperature (liquid helium) measurements of the temperature and field dependence of the paramagnetic MCD intensity, called ***C***-term intensity, are necessary. In this way, magnetic saturation curves can be detected optically [15,16], and, as detailed below, the fitting of these magnetization data allows for the determination of the polarizations of the observed transitions, *in samples of randomly oriented molecules* (i.e. not requiring single-crystal measurements) [17–21]. As demonstrated in this review, this information, combined with TD-DFT calculations, can be used to assign the optical spectra of metalloporphyrins, and in particular, identify charge-transfer transitions between the iron center of heme and the axial ligand(s) [21]. In addition, the total MCD intensity is very sensitive to the exact nature of the ground state, and can be correlated with changes in electron distribution of the iron center [22,23]. In comparison to UV–visible (UV–vis) spectroscopy, MCD has the additional advantage that MCD intensity is a signed quantity, and hence, a much better resolution of the optical transitions of metalloporphyrins is usually achieved with this technique. Compared to EPR spectroscopy, MCD is not restricted to non-integer spin systems.

In the following, these strengths of low-temperature MCD spectroscopy are used to investigate how the electronic properties of hemes can be fine-tuned via SCS effects in proteins. Useful complementary techniques to further support the conclusions drawn from MCD in terms of spectral assignments and ground state properties are EPR [24,25] and resonance Raman (rR) spectroscopy [26,27], and DFT calculations. Here we focus on high-spin ferrous and ferric hemes, since these are the (catalytically) active states of many heme proteins involved in $O_2$ and small molecule binding and activation.

## 2. Low-temperature MCD spectroscopy

The theoretical background of MCD spectroscopy was developed by P. J. Stephens in the 1970s and has been summarized in a number of reviews and articles [8,13,16,17,20,28,29]. MCD spectroscopy measures the difference in absorption of left (lcp) and right (rcp) circular polarized light in an applied, longitudinal magnetic field, usually generated by a superconducting magnet. MCD intensity arises from three different mechanisms, designated as MCD ***A***-, ***B***- and ***C***-terms, as shown in Eq. (1).

$$I \sim \left[A_1\left(\frac{-\partial f(E)}{\partial E}\right) + \left(B_0 + \frac{C_0}{kT}\right) f(E)\right] \cdot B \tag{1}$$

Here, $I$ is the MCD intensity, $T$ the temperature, $B$ the magnetic field and the function $f(E)$ represents the band shape of an absorption band. Importantly, the ***A***- and ***B***-terms are temperature independent, whereas MCD ***C***-term intensity is temperature dependent. Due to the $1/T$ dependence, the dominant mechanism at low temperature is in fact the ***C***-term. From Eq. (1), MCD intensity increases linearly with the strength of the magnetic field ($B$). This strictly applies to the ***A***- and ***B***-terms. On the other hand, ***C***-term intensity arises from a degenerate ground state, which is split in the applied magnetic field due to the Zeeman effect as shown in Scheme 1. Since the Jahn–Teller effect generally lifts orbital degeneracy of ground states, degenerate ground states usually originate from spin degeneracy, and hence, *only paramagnetic compounds exhibit **C**-term signals*.

At low temperatures, when kT is in the order of the Zeeman splitting in the presence of a strong magnetic field, a larger population of the lower energy compared to the higher energy Zeeman sublevels of the ground state results, according to the Boltzmann distribution. Hence, the intensities of the rcp and lcp transitions do not cancel anymore leading to an absorption band shape for the **C**-term. A further decrease of the temperature or an increase of the magnetic field results in an increase in the population of the lowest-energy sublevel and therefore, the **C**-term MCD intensity also increases. If the higher energy sublevels are completely depopulated, the **C**-term intensity reaches its maximum value, it saturates. Importantly, the temperature- and magnetic field-dependent **C**-term intensity (variable-temperature variable-field (VTVH) data) contains the complete information about the ground state properties including g values and zero-field splitting (ZFS) parameters, as well as the polarization of the respective electronic transition. All this information can be extracted by fitting these **C**-term saturation magnetization curves.

### 2.1. Fitting of variable-temperature variable-field (VTVH) MCD data

VTVH data obtained from the temperature- and field-dependent MCD ***C***-term intensity can be fitted using the general method developed by Neese and Solomon [18]. The analysis is based on the following Eq. (2):

$$\frac{\Delta\varepsilon}{E} = \frac{\gamma}{4\cdot\pi\cdot S}\int_0^{\pi}\int_0^{2\pi}\sum_i N_i\left(l_x\langle S_x\rangle_i M_{yz}^{eff} + l_y\langle S_y\rangle_i M_{xz}^{eff} + l_z\langle S_z\rangle_i M_{xy}^{eff}\right)\sin(\theta)\,d\theta\,d\phi \tag{2}$$

where the sum over $i$ runs over the sublevels of the ground state, $\Delta\varepsilon/E$ is the MCD intensity, $M^{eff}$ are the effective transition dipole moment products, $l$ are the angles between the magnetic field axes and the molecular coordinate system, $N_i$ are the Boltzmann populations, $\langle S\rangle_i$ are the spin-expectation values, $\gamma$ is a constant, and S is the total spin. The individual polarizations of MCD bands can then be calculated using the $M^{eff}$ values obtained from the fit of the VTVH saturation curves, using Eq. (3):

$$\%x = 100\cdot\frac{\left(M_{xy}^{eff}\cdot M_{xz}^{eff}\right)^2}{\left(M_{xy}^{eff}\cdot M_{xz}^{eff}\right)^2 + \left(M_{xy}^{eff}\cdot M_{yz}^{eff}\right)^2 + \left(M_{xz}^{eff}\cdot M_{yz}^{eff}\right)^2} \tag{3}$$

The calculation of the %y- and %z-polarization is performed correspondingly. This methodology is applied in the following to analyze the low-temperature MCD data of metalloporphyrins. In order to

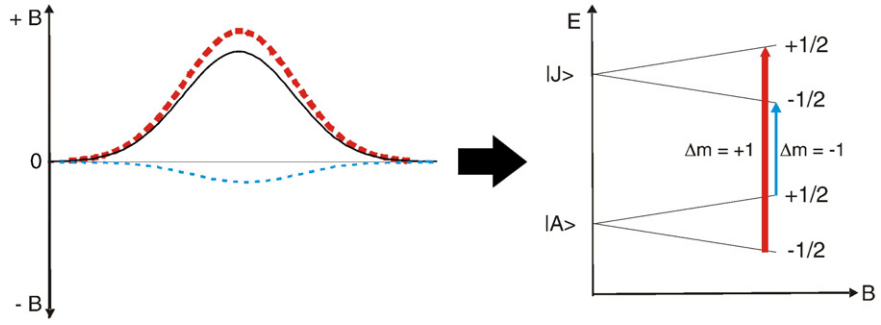


**Scheme 1.** MCD ***C***-term transition between the magnetically split sublevels of ground state |A> and excited state |J> for an S = 1/2 system.